The Meteoritical Society

Meteoritics & Planetary Science 43, Nr 4, 745–760 (2008)
Abstract available online at http://meteoritics.org

PDF orientations in shocked quartz grains around the Chicxulub crater

Yoichiro NAKANO[1], Kazuhisa GOTO[2*], Takafumi MATSUI[3], Ryuji TADA[1], and Eiichi TAJIKA[1]

[1]Department of Earth and Planetary Science, Graduate School of Science, The University of Tokyo, Build. #5, 7-3-1 Hongo, Tokyo 113-0033, Japan
[2]Tsunami Engineering Laboratory, Disaster Control Research Center, Graduate School of Engineering, Tohoku University, Aoba 06-6-11, Aramaki, Sendai 980-8579, Japan
[3]Department of Complexity Science and Engineering, Graduate School of Frontier Science, The University of Tokyo, 7-3-1 Hongo, Tokyo 113-0033, Japan
[*]Corresponding author. E-mail: kgoto@tsunami2.civil.tohoku.ac.jp

(Received 07 August 2006; revision accepted 04 September 2007)

Abstract–We measured 852 sets of planar deformation features (PDFs) in shocked quartz grains in impactite samples of the Yaxcopoil (YAX-1) core and from 4 Cretaceous/Tertiary (K/T) boundary deposits: the Monaca, the Cacarajícara, and the Peñalver formations in Cuba, and DSDP site 536, within 800 km of the Chicxulub crater, in order to investigate variations of PDF orientations in the proximity of the crater. Orientations of PDFs show a broad distribution with peaks at ω $\{10\bar{1}3\}$, π $\{10\bar{1}2\}$, and ξ $\{11\bar{1}2\}$, plus r, z $\{101\bar{1}\}$ orientations with minor c(0001), s$\{11\bar{2}1\}$, t$\{22\bar{4}1\}$ plus x$\{51\bar{6}1\}$, and m$\{10\bar{1}0\}$ plus a$\{11\bar{2}0\}$ orientations. Planar deformation features with c(0001) orientation are relatively more abundant in the proximity of the Chicxulub crater than in distal sites such as North America, the Pacific Ocean, and Europe. This feature indicates that in the proximity of the crater, part of the shocked quartz grains in the K/T boundary deposits were derived from the low shock pressure zones. Moreover, the orientations of PDFs with ξ $\{11\bar{2}2\}$ plus r, z $\{10\bar{1}1\}$ are high in our studied sites, and frequencies of these orientations decrease with increasing distance from the crater. On the other hand, absence of c(0001) and the rare occurrence of PDFs with ξ $\{11\bar{2}2\}$ plus r, z $\{10\bar{1}1\}$ orientations in the sample from the YAX-1 core that was taken at the top of the impactite layer of the Chicxulub crater suggests that the sampling horizon that reflects a certain cratering stage is also an important factor for variations in shocked quartz.

INTRODUCTION

Planar deformation features (PDFs) in shocked quartz grains are some of the most reliable evidence for impact phenomena on the Earth (e.g., French 1968). PDF orientations are used as a shock barometer because their crystallographic orientation varies with shock pressure (e.g., Grieve and Robertson 1976; Robertson and Grieve 1977; Langenhorst and Deutsch 1994; Grieve et al. 1996). Shocked quartz grains with PDFs in Cretaceous/Tertiary (K/T) boundary layers were first discovered by Bohor et al. (1984) and quartz grains with PDFs have been found at more than 50 K/T boundary sites worldwide (e.g., Claeys et al. 2002). Measurements of PDF orientations were conducted at only 13 sites (Bohor et al. 1984, 1987; Badjukov et al. 1986; Bostwick and Kyte 1996; Grieve and Alexopoulos 1988; Izett 1990; Sharpton et al. 1992; Kiyokawa et al. 2002; Tada et al. 2002), and there is no systematic study on the variation of PDF orientations among the K/T boundary sites. Moreover, the previous measurements of PDF orientations were conducted mainly at the K/T boundary sites in North America, the Pacific Ocean, and Europe (Fig. 1), located more than 3000 km away from the Chicxulub crater. Although shocked quartz grains with PDFs were also reported from the proximal K/T boundary sites around the Gulf of Mexico and the Caribbean Sea (e.g., Alvarez et al. 1992; Smit et al. 1992; Leroux et al. 1995; Pope et al. 1999; Takayama et al. 2000), very few measurements of PDF orientations have been conducted (Sharpton et al. 1992; Kiyokawa et al. 2002; Tada et al. 2002).

Shocked quartz grains with PDFs produced by the Chicxulub impact and distributed worldwide (e.g., Claeys et al. 2002; Morgan et al. 2006), provide us with a rare opportunity to study the distribution pattern of quartz grains with PDFs caused by a large impact event. Therefore, in order to investigate the distribution and variation of PDF orientations in the proximity of the Chicxulub crater, we measured PDF orientations in the following five sites, located up to 800 km from the center of the Chicxulub crater: the

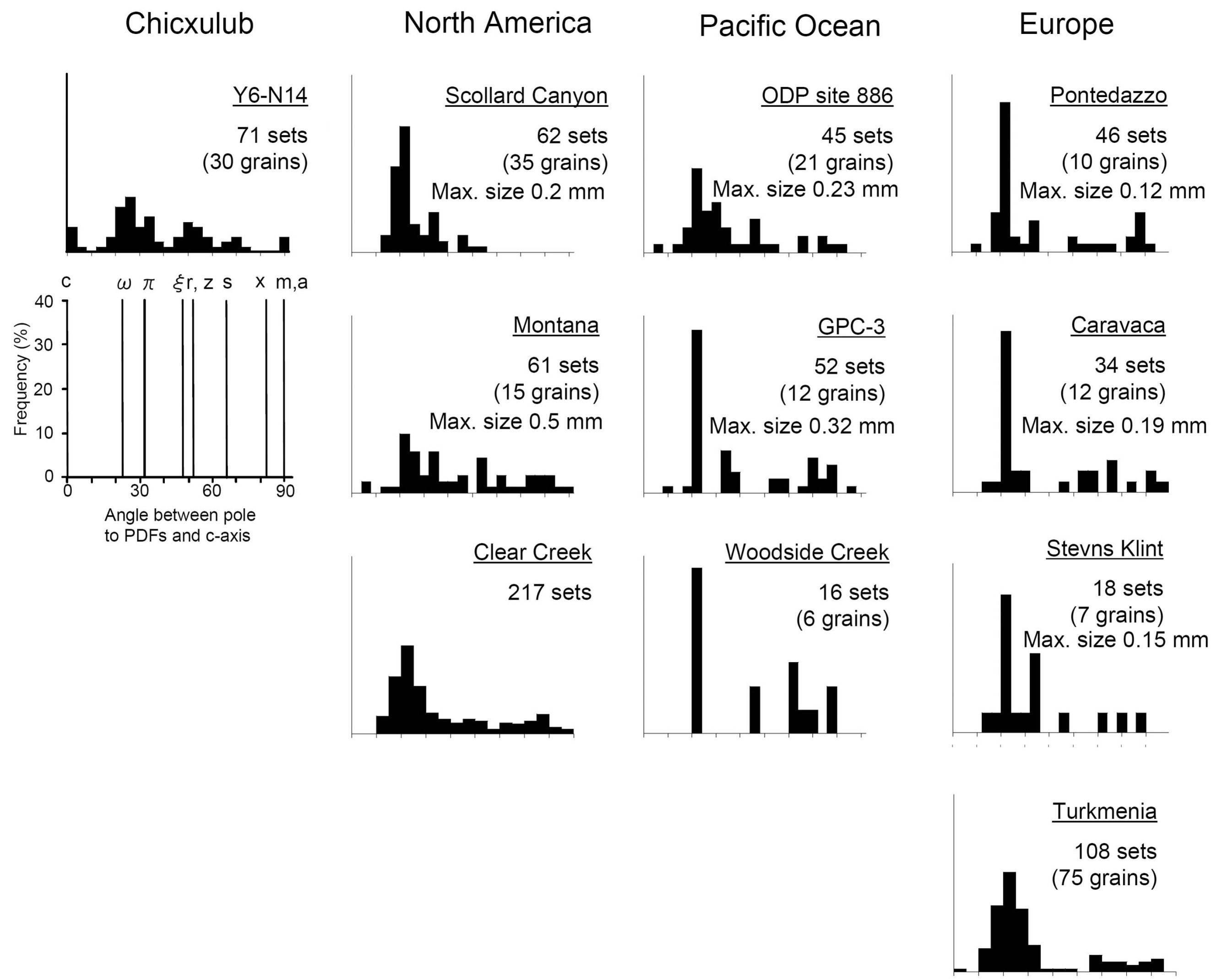

Fig. 1. Histograms showing the angle between the c-axis and pole to PDFs of the K/T boundary samples in North America, the Pacific Ocean, and Europe. Vertical axis of each histogram represents frequency (%). Maximum sizes of shocked quartz grains at each locality are also shown. Data for Pontedazzo, Caravaca, Stevns Klint, GPC-3, and Woodside Creek from Bohor et al. (1987), for Turkmenia from Badjukov et al. (1986); for ODP site 886 from Bostwick and Kyte (1996), for Scollard Canyon from Grieve and Alexopoulos (1988), for Montana from Bohor et al. (1984), for Clear Creek from Izett (1990), and for Y6-N14 from Sharpton et al. (1992).

ICDP drilling hole Yaxcopoil-1 (YAX-1) inside the crater, DSDP site 536, and the Moncada, the Cacarajícara and the Peñalver formations in Cuba (Fig. 2).

PREVIOUS STUDIES ON SHOCKED QUARTZ GRAINS

Since shock effects on quartz grains were discovered by DeCarli and Jamieson (1959), a number of studies have been carried out on shocked quartz (e.g., French and Short 1968; Langenhorst 1994; Langenhorst and Deutsch 1994; Stöffler and Langenhorst 1994; Gratz et al. 1996; Grieve et al. 1996; Vernooij and Langenhorst 2005). Shock-related effects in quartz are classified into 5 types: planar microstructures, mosaicism, high-pressure polymorphs (stishovite and coesite), diaplectic glass, and lechatelierite (French and Short 1968; Stöffler 1972, 1974; Alexopoulos et al. 1988; Sharpton and Grieve 1990; Stöffler and Langenhorst 1994; Grieve et al. 1996).

Planar microstructures are subdivided into planar fractures (PFs) and planar deformation features (PDFs) (e.g., Stöffler and Langenhorst 1994). Planar fractures are parallel open fissures, with spacing >20 μm and are formed at 5–7 GPa (Stöffler and Langenhorst 1994). Planar deformation features are single or multiple sets of parallel and planar lamellae, which is composed of amorphous silica or Brazil twins (Stöffler and Langenhorst 1994). PDFs are <3 μm thick and spaced with interval of <10 μm; they originate only in high dynamic regimes such as impact events, chemical and nuclear explosions, and shock experiments (Stöffler and Langenhorst 1994).

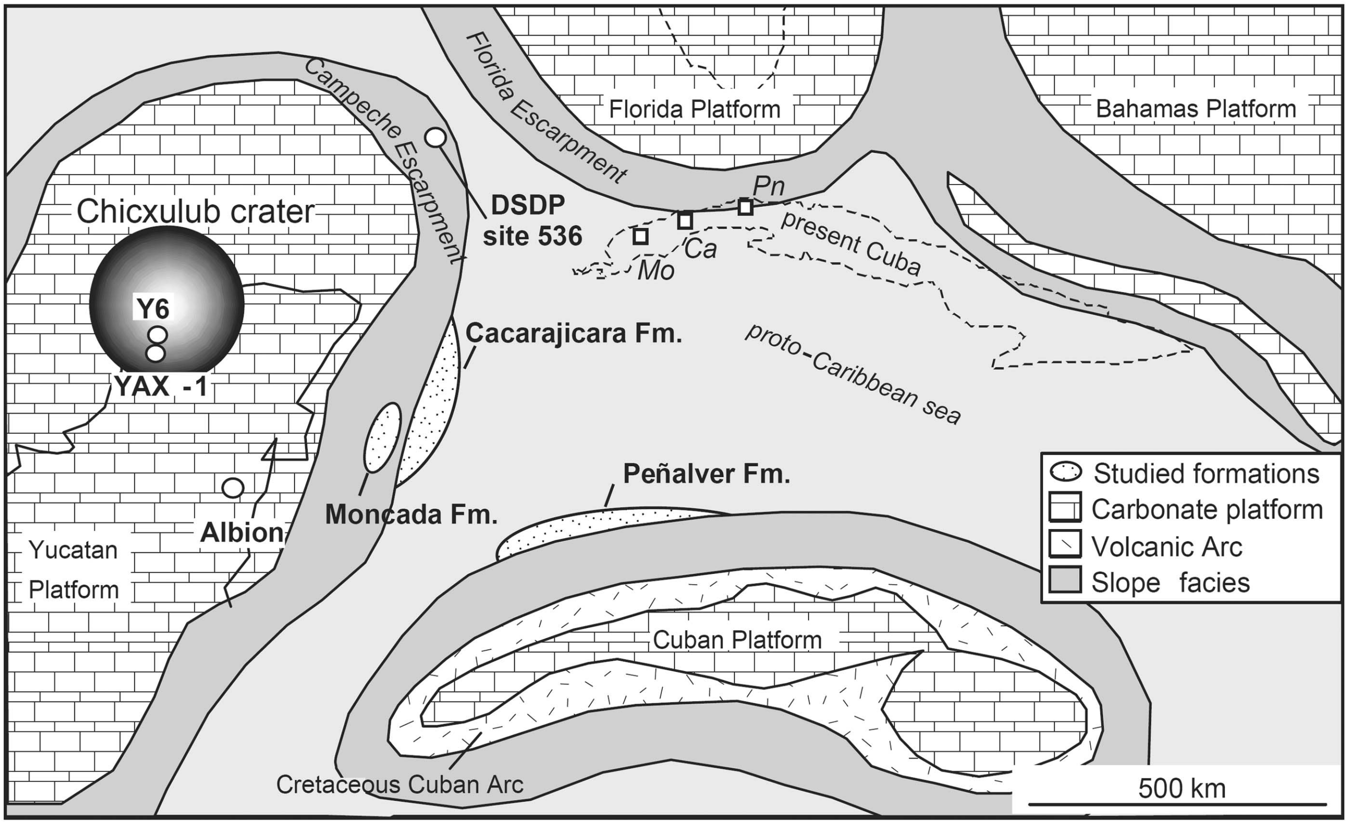

Fig. 2. Paleogeographic reconstruction of the studied area at the time of the K/T impact, 65 Ma ago (modified from Tada et al. 2003). Mo, Ca, Pn on the present Cuban island indicate the present position of the Moncada, Cacarajícara, and Peñalver Formations, respectively.

A number of experimental works on PDFs has been conducted since the first study of this type by Hörz (1968), and confirmed that PDFs develope at a shock pressure of >10 GPa (e.g., Stöffler and Langenhorst 1994). Based on the results of shock experiments on non-porous, crystalline target quartz (e.g., Hörz 1968), it is well known that PDF orientations vary with shock pressure intensity, and thus can be used as shock barometer (Table 1) (e.g., Robertson and Grieve 1977; Langenhorst and Deutsch 1994; Stöffler and Langenhorst 1994).

The PDF orientations in shocked quartz grains from a porous target are very different from those of the crystalline target (e.g., French et al. 1974; Grieve et al. 1996; Morrow and Sandberg 2001), yet the effect of porosity on development of PDFs is not well constrained. At some impact structures in a porous target such as the Oasis structure (French et al. 1974), PDFs are rare and a large proportion of the PDFs occurs at a high angle orientation such as $\xi\{11\bar{2}2\}$ and r, $z\{10\bar{1}1\}$.

GEOLOGICAL SETTING

At the end of the Cretaceous, 65 Ma ago, the proto-Caribbean Basin (Fig. 2) was bordered northward by the Florida Platform, northeastward by the Bahamian carbonate platform, westward by the Yucatán Platform, southward by the Cuban carbonate platform developed on the extinct Cretaceous Cuban Arc, and opened eastward to the Atlantic Ocean with the north-south width of over 500 km at the time of the K/T boundary impact (Pszczółkowski 1987; Rozencrantz 1990; Iturralde-Vinent 1994, 1998; Pindel 1994; Tada et al. 2003). The Cuban carbonate platform was probably located at 400–500 km to the south-southeast of its present position during the late Cretaceous (Rosencrantz 1990; Pindell 1994). The K/T boundary deposits accumulated under these paleogeographic configurations (Tada et al. 2003).

The ICDP (International Continental Scientific Drilling Program) Yaxcopoil-1 (YAX-1) drill hole is situated approximately 60 km to the south of the center of the Chicxulub crater (Fig. 2) in the depression between the rim and the central peak (Dressler et al. 2004). The DSDP site 536 is located approximately 500 km to the northeast of the center of the crater (Fig. 2), on a submarine ridge along the base of the Campeche Escarpment (Buffler et al. 1984; Alvarez et al. 1992).

The Moncada, Peñalver, and Cacarajícara formations in Cuba were deposited within the proto-Caribbean Sea (Fig. 2). The Moncada Formation was probably deposited on the continental slope on the eastern margin of the Yucatán Peninsula near the gateway between the Yucatán Platform and

Table 1. Shock pressures and PDF orientations dominated.

Approximate		Approximate	
Shock pressure (GPa)	Robertson and Grieve (1977)	Shock pressure (GPa)	Stöffler and Langenhorst (1994)
8.8	c (0001)	10–12	ω{1013}
12	ω {1013}	12–20	ω{1013}
15	ω{1013} with ξ {1122}, r, z {1011}		with s{1121}, ξ{1122}, m{1010}, {2131} and x{5161}
23	π {1012}	>20	π {1012}

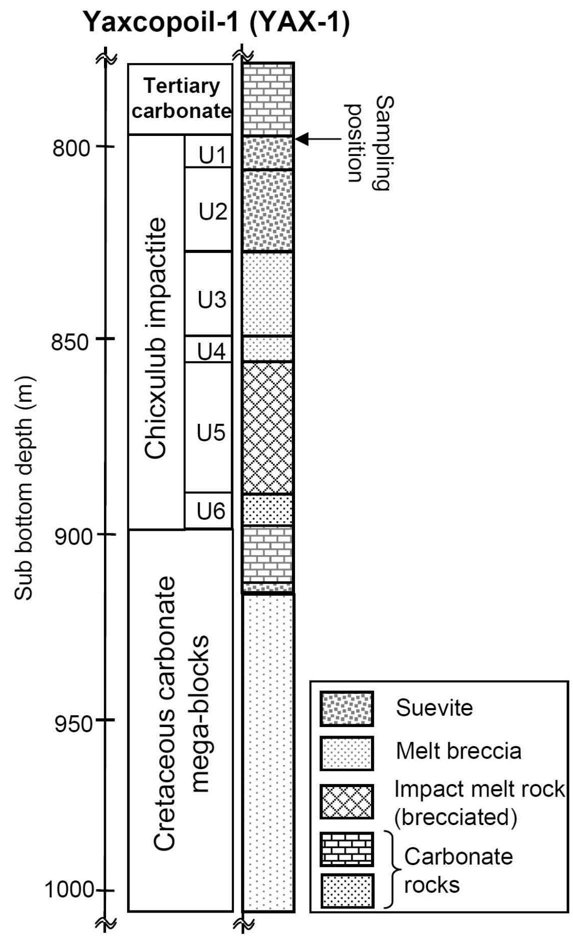

Fig. 3. Columnar section of the Yaxcopoil-1 core (modified from Goto et al. 2004) with giving the position of the sample investigated in this work.

the Cretaceous Cuban arc (Tada et al. 2002). The distance of the Moncada Formation from the center of the Chicxulub crater is approximately 500 km (Tada et al. 2002, 2003). The Cacarajícara Formation accumulated on the lower slope to basin floor on the eastern flank of the Yucatán Platform (Fig. 2) (Iturralde-Vinent 1994, 1998; Pszczółkowski 1999). The Cacarajícara Formation is considered to have been located approximately 500 km to the east of the center of the crater at the time of the K/T impact (Kiyokawa et al. 2002). The Peñalver Formation was deposited in a basin located on the slope on the north-northwest side of the Cuban carbonate platform (Fig. 2) (Iturralde-Vinent 1994, 1998) at approximately 600–2000 m water depth (Brönnimann and Rigassi 1963). The distance of the Peñalver Formation from the crater center is estimated at 500–800 km (Takayama et al. 2000).

STRATIGRAPHICAL SETTING AND SAMPLE HORIZONS

YAX-1

The YAX-1 drilling core is 1511 m in length, and from bottom to top, the core consists of ~600 m thick Cretaceous shallow water carbonate and sulfate rocks, ~100 m thick impactites, and ~800 m thick Tertiary carbonates (Fig. 3) (e.g., Dressler et al. 2004). Based on the lithology, Dressler et al. (2004) divided the impactite layers at Yax-1 into 6 units; units 6 to 1 in ascending order (Fig. 3). Each unit is interpreted as different forms of suevite, except for unit 5 (an impact melt breccia) (e.g., Dressler et al. 2004; Stöffler et al. 2004). Unit 1, composed of relatively well-sorted suevite with cross lamination at the top (e.g., Goto et al. 2004), is interpreted either as resurge deposit (Dressler et al. 2004; Goto et al. 2004) or a fall back ejecta deposit under dry condition with minor reworking at the top (Kring et al. 2004; Stöffler et al. 2004).

Shocked quartz grains with PDFs are reported in the impactite in each unit of the YAX-1 core (e.g., Goto et al. 2004; Smit et al. 2004; Stöffler et al. 2004; Tuchscherer et al. 2004). Tuchscherer et al. (2004) reported that shocked quartz grains in the YAX-1 core mainly have 1 to 3 sets of PDFs. They also reported more checkerboard feldspar in unit 4 than in all other units indicating shock pressures in excess of 45 GPa. In this study, we measured PDF orientation using one suevite sample from the top of unit 1 of the YAX-1 core (Fig. 3; 794.61 m in subbottom depth). This suevite is composed of greenish medium to coarse sandstone with cross lamination, and the sediments were probably deposited at the latest modification stage of the crater (Goto et al. 2004).

The Moncada Formation in Cuba

The Moncada Formation disconformably overlies the Albion-Cenomanian Pons Formation (Tada et al. 2002). It is a 2 m thick calcareous clastic deposit, divided into 6 units (Tada et al. 2002); units 1 to 5 and the uppermost unit (UMU) in ascending order (Fig. 4). The lower part of each unit is composed of a thicker, coarser-grained, parallel-laminated,

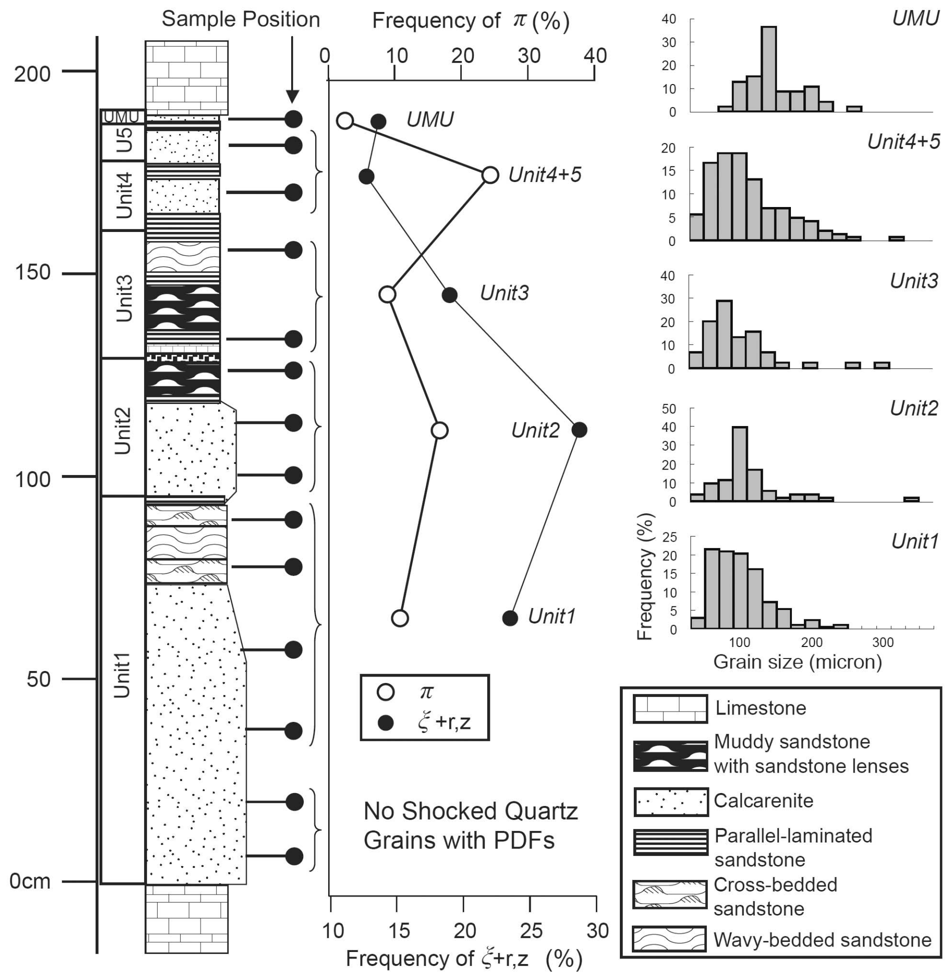

Fig. 4. A columnar section of the Moncada Formation. Sampling positions and vertical variations of frequency (%) of PDFs with π $\{10\bar{1}2\}$ and ξ $\{11\bar{2}2\}$ plus r, z $\{10\bar{1}1\}$ orientations are also shown. Frequency of PDFs with π $\{10\bar{1}2\}$ and ξ $\{11\bar{2}2\}$ plus r, z $\{10\bar{1}1\}$ is the average value of the samples in each unit. Grain size distributions in each unit are also shown in the right side. UMU = uppermost unit.

light-olive, calcareous sandstone, whereas the upper part is composed of alternations of thinner and finer-grained, parallel to ripple cross-laminated, light-gray calcareous sandstone and grayish-black mud drapes. The ripple cross-laminations at the top of each unit show north-south trending paleocurrent directions, which reversed several times, and are interpreted to have been formed by the repeated tsunamis (Tada et al. 2002). High iridium concentration peaks are observed both in the calcareous claystone of the UMU and the basal part of the Paleocene Ancón Formation, and these peaks were divided by a 1-cm-thick olive gray fine sandstone layer (Tada et al. 2002). This sandstone layer was probably formed by reworking after the start of deposition of Ir-bearing fine particles (Tada et al. 2002, 2003).

Shocked quartz grains with PDFs in the Moncada Formation were reported by Tada et al. (2002). In this study, we selected 14 samples from the Moncada Formation to cover the whole part of the formation (Fig. 4) in order to investigate the variation of PDF orientations over the section. The sample from the UMU was taken from the 1 cm thick sandstone layer in its upper part.

DSDP Site 536

Alvarez et al. (1992) divided the sedimentary sequence at DSDP sites 536 and 540 into 5 lithological units; units 1 to 5 in ascending order. Unit 1 is composed of autochthonous limestone of early Cenomanian age, and unit 2 is a 45 m thick pebbly mudstone of probable late Cenomanian age (Alvarez et al. 1992). Unit 3 is composed of calcirudite and calcarenite, and unit 4 is composed of calcilutite, and these units have distinct evidences of the K/T boundary impact event such as presence of spherules, shocked quartz grains, and an iridium anomaly (Alvarez et al. 1992; Bralower et al. 1998). Unit 5 conformably overlies unit 4, and is composed of planktonic foraminiferal ooze of Danian age (Alvarez et al. 1992).

At site 536, a sedimentary sequence from unit 1 to calcirudite part of unit 3 is not observed (Fig. 5). A sedimentary sequence from the calcarenite part of unit 3 to unit 5 is

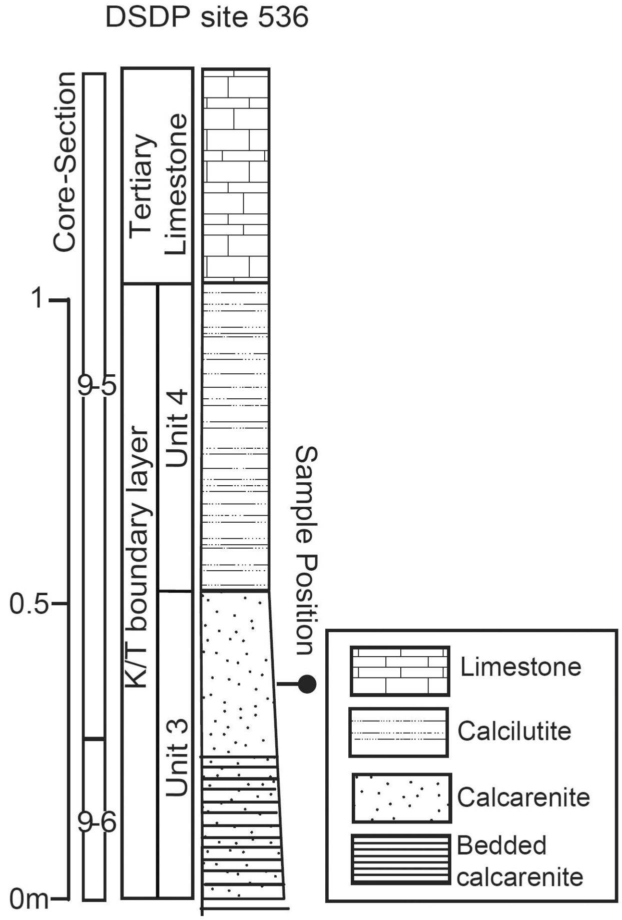

Fig. 5. Columnar section of the DSDP site 536 showing the position of the sample taken for this study.

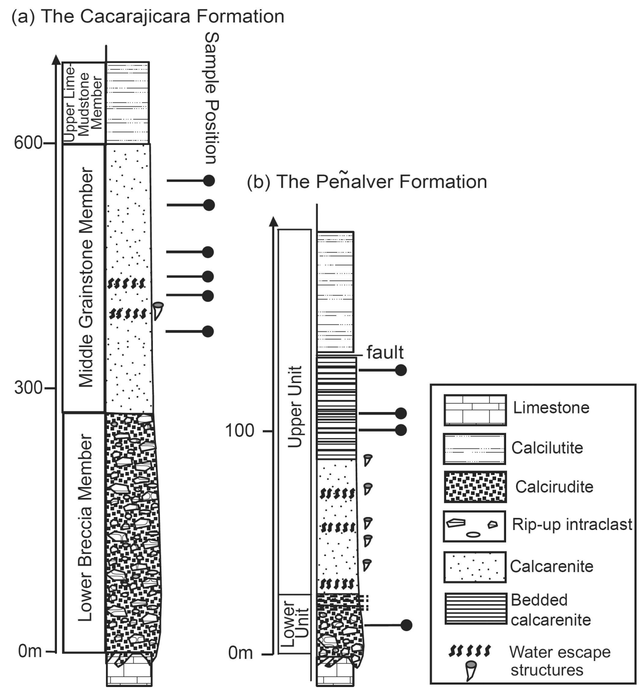

Fig. 6. Columnar sections of the Cacarajícara and the Peñalver formations in Cuba (modified from Takayama et al. 2000; Kiyokawa et al. 2002). Sampling positions are shown. Note different scales of the sections.

continuously recovered. The calcarenite part of unit 3 is 55 cm thick and is composed of hemipelagic to pelagic very fine- to fine-grained calcarenite. Calcarenite shows upward fining from a yellowish-green fine-grained base with several-centimeter-thick parallel bedding to whitish, massive, and very fine-grained top. The basal contact of unit 4 is gradational and conformable. Unit 4 is 50 cm thick and is composed of well-sorted, whitish massive calcilutite. The K/T boundary deposit in DSDP site 536 is interpreted as having been formed by the influence of tsunami and gravity flows (Alvarez et al. 1992; Bralower et al. 1998).

Shocked quartz grains were first reported at this site by Alvarez et al. (1992). In this study, we measured PDF orientation using one sample taken from the massive, and very fine-grained calcarenite part of unit 3 (Fig. 5; core 9–5, 123–125 cm).

The Cacarajícara Formation in Cuba

The Cacarajícara Formation is a 700 m thick calcareous clastic deposit, which is composed of 3 lithological members (Fig. 6): Lower Breccia (LBM), Middle Grainstone (MGM), and Upper Lime-mudstone (ULM) members in ascending order (Kiyokawa et al. 2002; Tada et al. 2003). The approximately 250 m thick LBM is composed of limestone and chert boulders and is interpreted as being formed by laminar flow from the Yucatán Platform triggered by earthquakes due to the cratering event (Kiyokawa et al. 2002). The approximately 450 m thick MGM and ULM consists of upward graded, massive to well-bedded, homogeneous calcarenite and fine calcareous mudstone without any bioturbation. These members may have been formed by a turbidite and a low-density turbidite, respectively, associated with the laminar flow deposit of the LBM (Kiyokawa et al. 2002) and by the tsunami associated with the impact (Tada et al. 2003).

Shocked quartz grains with PDFs were reported from every member of the Cacarajícara Formation by Kiyokawa et al. (2002). In this study, we measured PDF orientations using 6 samples taken from the MGM (Fig. 6).

The Peñalver Formation in Cuba

The Peñalver Formation is a more than 180 m thick calcareous clastic deposit, composed of a lower and an upper unit (Fig. 6). The lower 30 m (Lower Unit) is composed of calcirudite derived from a shallow platform on the Cuban volcanic arc and is considered to have been formed by debris flows triggered by the impact-related earthquake (Takayama et al. 2000). The upper 150 m (Upper Unit) are composed of calcarenite and calcilutite layers without sedimentary structures indicative of current, and these layers are considered to have been formed under the influence of tsunami (Takayama et al. 2000; Tada et al. 2003; Goto et al. 2008).

Shocked quartz grains with PDFs were reported both from the Lower and Upper units at the type locality by Takayama et al. (2000) and Goto et al. (2002). In this study, we measured PDF orientations using 1 sample from the Lower Unit and 3 samples from the calcarenite part of the Upper Unit (Fig. 6).

ANALYTICAL METHOD

We concentrated quartz grains by the following procedures. Because the studied samples are highly calcareous, we first treated the samples with hydrochloric acid (6N HCl) for 12 h in order to dissolve the carbonate fraction. The insoluble residue was washed 3 to 5 times to decant the clay minerals. Then, the insoluble residue was treated with 30% hydrofluosilicic acid (H_2SiF_6) for 1 to 2 weeks to dissolve silicate minerals except for quartz grains (Takayama et al. 2000). Because hydrofluorosilicic acid dissolves amorphous silica that fills the PDFs, PDFs can be easily identified by a scanning electron microscope (SEM) without etching them by hydrogen fluoride (HF). After these treatments, almost all the residue was composed of quartz grains. Because PDFs in shocked quartz grains smaller than 30 µm are difficult to identify as mentioned by Bostwick and Kyte (1996), we split silicate grains smaller than 32 µm using a sieve. Final residues were mounted on glass plates with epoxy resin, and thin sections were prepared. Shocked quartz grains larger than 32 µm with PDFs were observed under the microscope and SEM. We investigated a maximum grain size of shocked quartz grain in each sample as an indicator of grain size. For the Moncada Formation, we also investigated the grain size distributions of shocked quartz grains. We also measured the abundance of shocked quartz grains relative to the total quartz grain in each sample.

Orientations of PDFs were measured by using a universal stage based on the method of Langenhorst (2002). Precision of measurement of PDF orientations was ±5°. As will be mentioned below, PDFs with ξ $\{11\bar{2}2\}$ and r, z $\{10\bar{1}1\}$ orientations are characteristically observed in our samples. However, it is difficult to separate ξ $\{11\bar{2}2\}$ from r, z $\{10\bar{1}1\}$, because difference in orientations of these two planes is smaller than the measurement precision (Table 2). Therefore, these orientations are not separated but are described as ξ $\{11\bar{2}2\}$ plus r, z $\{10\bar{1}1\}$. In the same manner, we described PDFs with t$\{22\bar{4}1\}$ and x$\{5161\}$ orientations as t$\{2241\}$ plus x$\{5161\}$.

RESULTS

Quartz grains with PDFs were found in the samples from all the studied sites except for the basal 2 samples of unit 1 of the Moncada Formation. The lamellae in shocked quartz grains are single or multiple sets of parallel and planar optical discontinuities (Fig. 7a). The observation with SEM revealed that the lamellae are <1 µm thick with a spacing of <10 µm (Fig. 7b).

Figure 8 shows histograms of the angle between c-axis and pole to PDFs for the studied localities. Furthermore, measured angles of PDFs, which are within ±5° from the theoretical orientations (c(0001), ω $\{10\bar{1}3\}$, π $\{10\bar{1}2\}$, ξ$\{11\bar{2}2\}$ plus r, z $\{10\bar{1}1\}$, s$\{11\bar{2}1\}$, t$\{2\bar{2}41\}$ plus x$\{5\bar{1}61\}$, and m$\{10\bar{1}0\}$ plus a$\{11\bar{2}0\}$), are indexed following Grieve et al. (1996) (Table 2).

YAX-1

We investigated 48 shocked quartz grains in 1 sample taken from top of the unit 1 of the YAX-1 core and found 80 sets of PDFs. Up to 5 sets of PDFs are observed in a single quartz grain (Table 3), approximately 31% of all quartz grains are shocked. Their maximum grain size is 300 µm.

Planar deformation features with ω $\{10\bar{1}3\}$, π $\{10\bar{1}2\}$, ξ $\{11\bar{2}2\}$ plus r, z $\{10\bar{1}1\}$, s$\{11\bar{2}1\}$, t$\{22\bar{4}1\}$ plus x$\{51\bar{6}1\}$, and m$\{10\bar{1}0\}$ plus a$\{11\bar{2}0\}$ orientations are observed in this sample (Fig. 8 and Table 2), whereas PDF with c(0001) orientation is not observed. Planar deformation features with ω $\{10\bar{1}3\}$, π $\{10\bar{1}2\}$ and s$\{11\bar{2}1\}$ orientations are the major components in this sample (26, 20, and 20%, respectively), whereas PDFs with ξ $\{11\bar{2}2\}$ plus r, z $\{10\bar{1}1\}$ orientation represent 1% (Table 2). Frequencies of PDFs with t$\{22\bar{4}1\}$ plus x$\{51\bar{6}1\}$, and m$\{10\bar{1}0\}$ plus a$\{11\bar{2}0\}$ orientations are less than 11% (Table 2).

The Moncada Formation

There are 335 sets of PDFs in 233 shocked quartz grains in the upper 12 samples, whereas no shocked quartz grain has been found in the basal 2 samples (Fig. 3). Up to 4 sets of PDFs are observed in a single quartz grain (Table 3). Abundance of shocked quartz grains is less than 27% (Table 3).

The maximum grain size of shocked quartz is 240 µm for unit 1, 340 µm for unit 2, 300 µm for unit 3, 320 µm for units 4 + 5, and 260 µm for UMU (Table 3). Grain size of shocked quartz shows a broad distribution in each unit from <32 µm to 240–340 µm (Fig. 4). Average grain size is 100–110 µm in units 1 to 4 + 5 and 150 µm in UMU.

Planar deformation features with c(0001), ω $\{10\bar{1}3\}$, π $\{10\bar{1}2\}$, ξ $\{11\bar{2}2\}$ plus r, z $\{10\bar{1}1\}$, s$\{11\bar{2}1\}$, t$\{22\bar{4}1\}$ plus x$\{5161\}$, and m$\{10\bar{1}0\}$ plus a$\{11\bar{2}0\}$ orientations are observed in the Moncada Formation (Fig. 8 and Table 2). Among these, PDFs with ω $\{10\bar{1}3\}$, ξ$\{11\bar{2}2\}$ plus r, z $\{10\bar{1}1\}$, and π $\{10\bar{1}2\}$ orientations are the prominent components (Table 2). Over the section, the frequency of PDFs with ξ $\{11\bar{2}2\}$ plus r, z $\{10\bar{1}1\}$ decreases upwards from approximately 29 to 13% (Fig. 4), whereas PDFs with ω $\{10\bar{1}3\}$ shows an upward increasing trend from approximately

Table 2. Indexed angles of PDFs in shocked quartz grains in the studied area.[a]

Locality	Sample horizon	c 0.00[b] frequency (%)	ω 22.95 frequency (%)	π 32.45 frequency (%)	ξ + r,z 47.73, 51.79 frequency (%)	s 65.56 frequency (%)	t + x 78.87, 82.07 frequency (%)	m,a 90.00 frequency (%)	Unindexed frequency (%)
YAX-1	(794.61 m)	n.d.*[c]	26.3	20.0	1.3	20.0	11.3	2.5	18.6
DSDP 536	(9–5, 123–125 cm)	2.9	43.1	6.9	13.7	5.9	11.7	2.9	12.9
Cacarajicara Fm.	(MGM*[d])	1.4	37.1	14.3	10.0	5.7	5.7	4.3	21.5
Peñalver Fm.	(Lower Unit)	1.3	29.1	17.7	15.2	6.3	10.1	5.1	15.2
Peñalver Fm.	(Upper Unit)	5.3	39.4	12.8	17.6	4.3	3.7	2.1	14.9
Moncada Fm.	(Unit 1)	7.0	39.5	10.5	23.3	11.6	2.4	3.5	2.2
Moncada Fm.	(Unit 2)	1.1	24.5	16.0	28.7	9.6	6.4	5.3	8.4
Moncada Fm.	(Unit 3)	2.1	43.8	8.3	18.8	6.3	10.5	4.2	6.0
Moncada Fm.	(Unit 4 + 5)	2.1	37.5	25.0	12.6	10.4	4.2	4.2	4.0
Moncada Fm.	(UMU[e])	6.8	55.9	1.7	13.6	6.8	6.8	n.d.	8.4

[a]Measured angles of PDFs, which are within ±5° from the theoretical orientations, are indexed in this table. Note that mode of expression is different from Fig. 8 (see details in Grieve et al. 1996).
[b]Angle between pole to PDFs and c-axis.
[c]Not detected.
[d]Middle Grainstone member.
[e]Uppermost unit.

25 to 56%. Planar deformation features with π $\{10\bar{1}2\}$ orientation shows upward increasing trend from approximately 11 to 25% from units 1 to 4 + 5, but it is approximately 2% in the UMU (Fig. 4). Planar deformation features with a high angle to the c-axis (>60°) are also observed (Table 2): the frequency of PDFs with s$\{11\bar{2}1\}$ orientation is approximately 6–12%, whereas frequency of PDFs with t$\{2\bar{2}41\}$ plus x$\{5\bar{1}61\}$, and m$\{10\bar{1}0\}$ plus a$\{1\bar{1}20\}$ are less than 11% (Table 2). No systematic variations over the section are observed in these orientations.

DSDP Site 536

There are 102 sets of PDFs in 73 grains in the one sample from the calcarenitic part of unit 3. Up to 3 sets of PDFs are observed in a single quartz grain (Table 3). The abundance of shocked quartz grains is approximately 16% of total quartz grains. The maximum grain size of shocked quartz grains is 140 µm and, hence, significantly smaller than that in the other studied sites.

In this sample, PDFs with c(0001), ω $\{10\bar{1}3\}$, π $\{10\bar{1}2\}$, ξ $\{11\bar{2}2\}$ plus r, z $\{10\bar{1}1\}$, s$\{11\bar{2}1\}$, t$\{22\bar{4}1\}$ plus x$\{51\bar{6}1\}$, and m$\{10\bar{1}0\}$ plus a$\{11\bar{2}0\}$ orientations are observed (Fig. 8 and Table 2). Planar deformation features with ω $\{10\bar{1}3\}$ and ξ $\{11\bar{2}2\}$ plus r, z $\{10\bar{1}1\}$ orientations are the prominent components (43% and 14%, respectively). Frequencies of PDFs with a high angle to the c-axis (>60°) are less than 12% (Table 2).

The Cacarajícara Formation

There are 68 sets of PDFs in 49 grains of the 6 samples taken from the Middle Grainstone Member. Up to 4 sets of PDFs are observed in a single quartz grain (Table 3). Abundance of shocked quartz grains is less than 2% of total quartz grains. The maximum grain size of shocked quartz grain is 410 µm.

PDFs with c(0001), ω $\{10\bar{1}3\}$, π $\{10\bar{1}2\}$, ξ $\{11\bar{2}2\}$ plus r, z $\{10\bar{1}1\}$, s$\{11\bar{2}1\}$, t$\{22\bar{4}1\}$ plus x$\{51\bar{6}1\}$, and m$\{10\bar{1}0\}$ plus a$\{11\bar{2}0\}$ orientations are observed (Fig. 8 and Table 2). Planar deformation features with ω $\{10\bar{1}3\}$, π $\{10\bar{1}2\}$ and ξ $\{11\bar{2}2\}$ plus r, z $\{10\bar{1}1\}$ orientations are the prominent components and their frequencies are 37, 14, and 10%, respectively (Table 2). Frequencies of PDFs with a high angle to the c-axis (>60°) are less than 6% (Table 2).

The Peñalver Formation

There are 79 sets of PDFs in 59 grains in the sample from the Lower Unit and 188 sets in 132 grains in 3 samples from the Upper Unit. Up to 3 and 4 sets of PDFs are observed in a single quartz grain in samples from the Lower and Upper units (Table 3), respectively. Abundance of shocked quartz grains are approximately <1 and 2% of total quartz grains, respectively. The maximum grain sizes of shocked quartz grain in each unit are 320 and 380 µm, respectively.

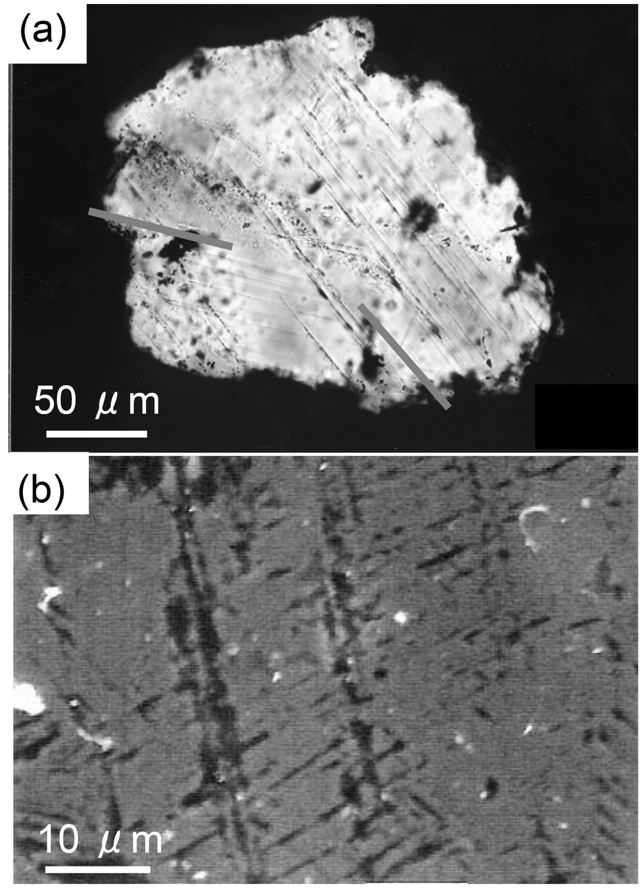

Fig. 7. a) Shocked quartz grain with PDFs in the middle part of the Moncada Formation (cross-polarized light). b) SEM image of shocked quartz grain in the Moncada Formation. PDFs are <1 µm thick with a spacing of <10 µm. The sample was treated with hydrofluosilicic acid.

In the samples from the Lower and Upper units, PDFs with c(0001), ω $\{10\bar{1}3\}$, π $\{10\bar{1}2\}$, ξ$\{11\bar{2}2\}$ plus r, z $\{10\bar{1}1\}$, s$\{11\bar{2}1\}$, t$\{22\bar{4}1\}$ plus x$\{51\bar{6}1\}$, and m$\{10\bar{1}0\}$ plus a$\{11\bar{2}0\}$ orientations are observed (Fig. 8 and Table 2). PDFs with ω $\{10\bar{1}3\}$, π $\{10\bar{1}2\}$ and ξ $\{11\bar{2}2\}$ plus r, z $\{10\bar{1}1\}$ orientations are the prominent components and their frequencies are 29, 18, and 15% in the Lower Unit, and 39, 13, and 18% in the Upper Unit, respectively (Table 2). Frequencies of PDFs with high angle (>60°) are less than 10% in the Lower Unit and 4% in the Upper Unit, respectively.

DISCUSSION

Abundance of Shocked Quartz Grains

Bostwick and Kyte (1996) reported that in average 63% of all quartz grains are shocked quartz at K/T boundary deposits in the Pacific Ocean sites, although Morgan et al. (2006) recently reported a fewer amount of shocked quartz grains in

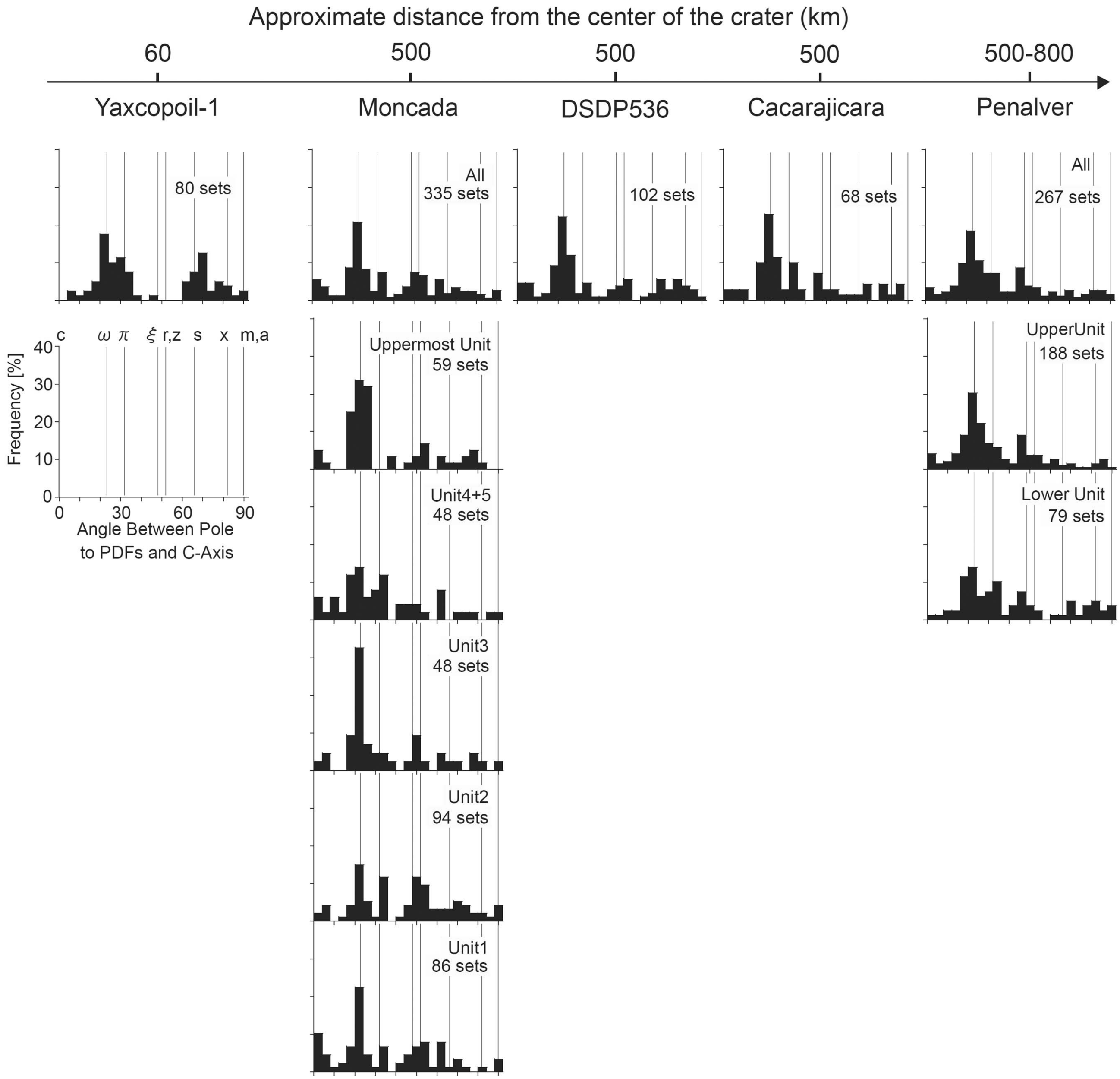

Fig. 8. Histograms showing the angle between c-axis and pole to PDFs for the studied localities.

these sites. Because the K/T boundary layers in the Pacific Ocean sites are approximately 3 mm thick, and reworked local sediments are not significant, shocked quartz grains were probably not diluted by the local detrital quartz grains. Thus, it is possible in this case to estimate the proportion of shocked to non-shocked quartz grains in ejecta materials (Bostwick and Kyte 1996).

On the other hand, the abundance of shocked quartz grains is approximately 31% in the impactite sample of the Yax-1, 16% in the sample from the DSDP site 536, and 19–27% in the samples from the Moncada Formation. The abundance of shocked quartz grains at the Peñalver and Cacarajícara formations is very low (<2%). These values are significantly low compared to those at the Pacific Ocean sites. Considering the large thickness of K/T boundary deposits at our studied sites (~700 m) and the presence of a large amount of reworked sediments (e.g., Tada et al. 2003), low abundance of shocked quartz grains at these sites is probably explained by the extensive dilution by the local detrital quartz grains (e.g., Claeys et al. 2002).

Mean and Maximum Sizes of Shocked Quartz Grains

Grain size of shocked quartz at the Moncada Formation ranges from <32 to 340 μm with mean sizes from 100 to 150 μm. This mean size compares well to that in Haiti (80–160 μm)

Table 3. Abundance, maximum grain size, and number of PDFs in one grain at studied K/T sites.

Locality	Sample horizon	Percent quartz with PDFs (%)	Largest quartz grain with PDFs (μm)	PDF number in one grain (%)				
				1 set	2 sets	3 sets	4 sets	5 sets
YAX-1	794.61 m	31	300	50	38	10	0	2
DSDP 536	9–5, 123–125 cm	16	140	62	34	4	0	0
Cacarajícara Fm.	MGM*[a]	2	410	66	26	6	2	0
Peñalver Fm.	Lower Unit	<1	320	69	27	3	0	0
Peñalver Fm.	Upper Unit	2	380	68	23	8	2	0
Moncada Fm.	Unit 1	23	240	65	28	2	5	0
Moncada Fm.	Unit 2	19	340	60	19	15	6	0
Moncada Fm.	Unit 3	27	300	83	13	0	4	0
Moncada Fm.	Unit 4 + 5	23	320	76	21	3	0	0
Moncada Fm.	UMU*[b]	27	260	82	18	0	0	0

[a]Middle Grainstone member.
[b]Uppermost unit.

(Kring et al. 1994; Leroux et al. 1995) and North America (60–200 μm) (Grieve and Alexopoulos 1988; Izett 1990; Morgan et al. 2006), but is larger than at the Pacific Ocean (<50–70 μm) (Bostwick and Kyte 1996; Morgan et al. 2006), and Atlantic Ocean sites (40 μm) (Morgan et al. 2006), and at European localities (<60 μm) (Morgan et al. 2006). As is stated by Bohor (1990) and Morgan et al. (2006), the mean size of shocked quartz grain seems to decrease with increasing distance from the Chicxulub crater.

The maximum size in each site also gives useful information for discussing the geographical distribution of shocked quartz grains (e.g., Claeys et al. 2002). It is, however, important to evaluate whether the maximum size is representative for the site (e.g., Bostwick and Kyte 1996; Claeys et al. 2002). Because the K/T boundary layer around the Gulf of Mexico and proto-Caribbean Sea is exceptionally thick (e.g., Smit 1999; Tada et al. 2003), a large number of samples from different horizons should be investigated to estimate a representative maximum size at each site. For example, the maximum grain sizes are 300 and 140 μm in the samples from the YAX-1 core and the DSDP site 536. However, we believe that these sizes may not be representative for those sites, because the investigated sample amounts are very small, whereas the thickness of the impactite layer of the YAX-1 and the K/T boundary layer of the DSDP site 536 is 100 m and >2 m respectively. In the same manner, at the Moncada, Cacarajícara, and the Peñalver formations, the number of measured samples was small considering the large thicknesses of these deposits. Therefore, the true maximum sizes at these sites should be larger than those observed.

Variation of PDF Orientations of Shocked Quartz Grains

In this study, we measured 852 PDF orientations in quartz grains at the 5 sites within 800 km of the center of the Chicxulub crater. Up to 5 sets of PDFs were identified in one quartz grain at the studied sites (Table 3). The orientations of PDFs in quartz grains at each studied site show a broad distribution with high peaks at ω $\{10\bar{1}3\}$, π $\{10\bar{1}2\}$, and ξ $\{11\bar{2}2\}$ plus r, z $\{10\bar{1}1\}$ (Fig. 8). Broad distribution patterns of PDF orientations are similar to those reported for samples from the Yucatán 6 (Y6) site drilled inside the crater (Sharpton et al. 1992), but are quite different from those at distal sites such as North America, Pacific Ocean, and Europe (Fig. 1); there are high peaks at ω $\{10\bar{1}3\}$ and π $\{10\bar{1}2\}$ orientations with rare frequencies of other orientations.

Combination of PDFs derived from low (e.g., PDFs with c(0001)) and high (e.g., PDFs with π $\{10\bar{1}2\}$) shock pressures in a single grain is rare. Therefore, broad distributions of PDF orientation in our samples suggest that the shocked quartz grains derived from zones from different shock levels. Thus, difference in PDF orientations among the sites and among different sampling horizons may provide useful information to understand the ejection process of shocked quartz grains. In fact, there are characteristic variations in frequencies of PDFs with c(0001) and ξ $\{11\bar{2}2\}$ plus r, z $\{10\bar{1}1\}$ orientations as discussed below.

Frequency of PDFs with c(0001) Orientation

It has been pointed out that there are almost no PDFs with c(0001) orientation in the K/T boundary deposits of Europe, North America, and the Pacific Ocean (Fig. 1) (Grieve and Alexopoulos 1988; Bostwick and Kyte 1996; Grieve et al. 1996). On the other hand, shocked quartz grains in the samples from the DSDP site 536, the Cacarajícara, the Moncada, and the Peñalver formations contain PDFs with c(0001), although the frequency is less than 7%.

Because PDFs with c(0001) orientation is formed under the lowest shock pressure (Table 1) (Robertson and Grieve 1977), the occurrence of such a PDF orientation in the samples at DSDP site 536, the Cacarajícara, the Moncada, and the Peñalver formations probably suggests that K/T boundary deposits in these sites contain shocked quartz grains derived from lower shock pressure zones compared to those in Europe, North America, and the Pacific Ocean. According to Melosh (1989) and Alvarez et al. (1995), the central part of the crater is subject to high shock pressure (high shock pressure zone (HSPZ)), and materials are ejected with high

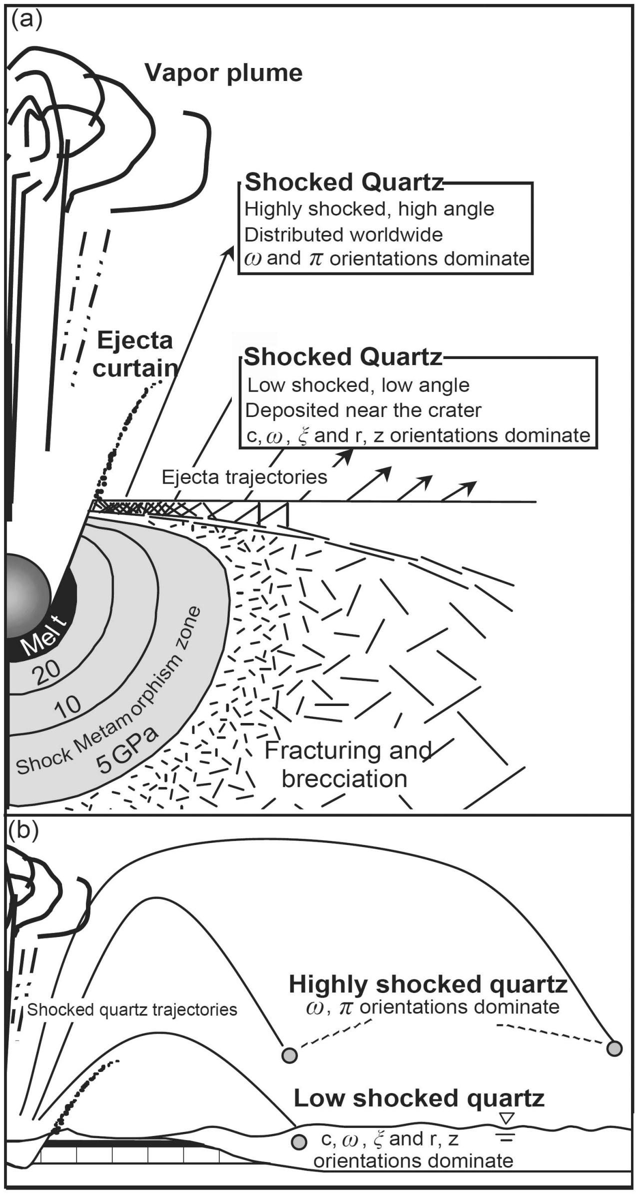

Fig. 9. a) An illustration of the ideal crater formation model modified from Melosh (1989). Shocked quartz grains produced in the central part of the crater could have been ejected at high speed and a high angle, whereas shocked quartz grains produced around outer zone of the growing crater could have been ejected with low speed and low angle and thus distributed near the crater. Planar deformation features with c(0001), ξ {11$\bar{2}$2} plus r, z {10$\bar{1}$1} orientations, which were probably formed under the low-shock pressure zone, are abundant in the proximity of the crater. b) An illustration of the settling process of shocked quartz grains through the atmosphere and the ocean. Shocked quartz grains produced by low shock pressure probably settled faster than those produced by high shock pressure (based on Alvarez et al. 1995).

angle and high speed (Fig. 9a). On the other hand, the outer zone of the growing crater is subject to lower shock pressure (low shock pressure zone (LSPZ)), and materials are ejected with low angle and low speed (Melosh 1989; Alvarez et al. 1995). According to this model, it is considered that shocked quartz grains derived from the LSPZ were deposited closer to the crater, whereas shocked quartz grains derived from the HSPZ were distributed worldwide (e.g., ejecta curtain versus warm fireball zones in Alvarez et al. 1995). The variation in frequency of PDFs with c(0001) orientation in the K/T boundary layers observed in this study is consistent with this model.

On the contrary, the sample from the YAX-1 core does not contain PDFs with c(0001) orientation (Table 2), suggesting that the presence of PDFs with c(0001) cannot be explained only by the distance from the crater. Absence of PDFs with c(0001) in the sample from the YAX-1 is probably related to the sampling horizon that reflects the depositional stage of shocked quartz grains. Because shocked quartz grains derived from the HSPZ could have been ejected to the higher level of the atmosphere, they could have been deposited well after the deposition of shocked quartz derived from the LSPZ (Fig. 9b) (Alvarez et al. 1995; Stöffler et al. 2004). The studied sample from the YAX-1 core was taken from the top of the impactite layer and the sediments in this horizon were probably formed during the latest modification stage of the crater (e.g., Goto et al. 2004). Therefore, it is possible to interpret that shocked quartz grains derived from the HSPZ probably dominated in this horizon without shocked quartz grains derived from the LSPZ. This is probably the reason why the sample from the YAX-1 core does not contain PDFs with c(0001) orientation.

Of note, Sharpton et al. (1992) reported approximately 7% of PDFs with c(0001) from the suevite sample (Y6-N14) of the Y6 core, approximately 50 km from the center of the crater. The suevite layer in the Y6 core is more than 150 m thick, and is composed of lower, middle, and upper suevite units (Claeys et al. 2003). The Y6-N1 4 sample was located in the middle pebbly suevite unit (1208–1211 m subbottom depth), and this unit is interpreted to have been deposited out of the ejecta plume as fall-back material (Claeys et al. 2003; Claeys 2006). Therefore, suevite in this unit was deposited apparently before the deposition of the suevite at our sampling horizon of the YAX-1 core, and might have been deposited within the order of minutes to hours after the impact. Although a further detailed investigation using more impactite samples from different horizons is required, presence of PDFs with c(0001) in Y6-N14 sample together with the absence of c(0001) in our sample from the YAX-1 may suggest that the depositional stage of shocked quartz grains is also an important factor affecting variation in PDF orientation.

Frequency of PDFs with ξ {11$\bar{2}$2} Plus r, z {10$\bar{1}$1} Orientations

The studied samples at DSDP site 536, the Cacarajícara, the Moncada, and the Peñalver formations contain 10–29% of PDFs with ξ {11$\bar{2}$2} plus r, z {10$\bar{1}$1} orientation, although the sample from the YAX-1 core contains only 1% (Table 2 and Fig. 8). The frequency of PDFs with ξ {11$\bar{2}$2} plus r, z

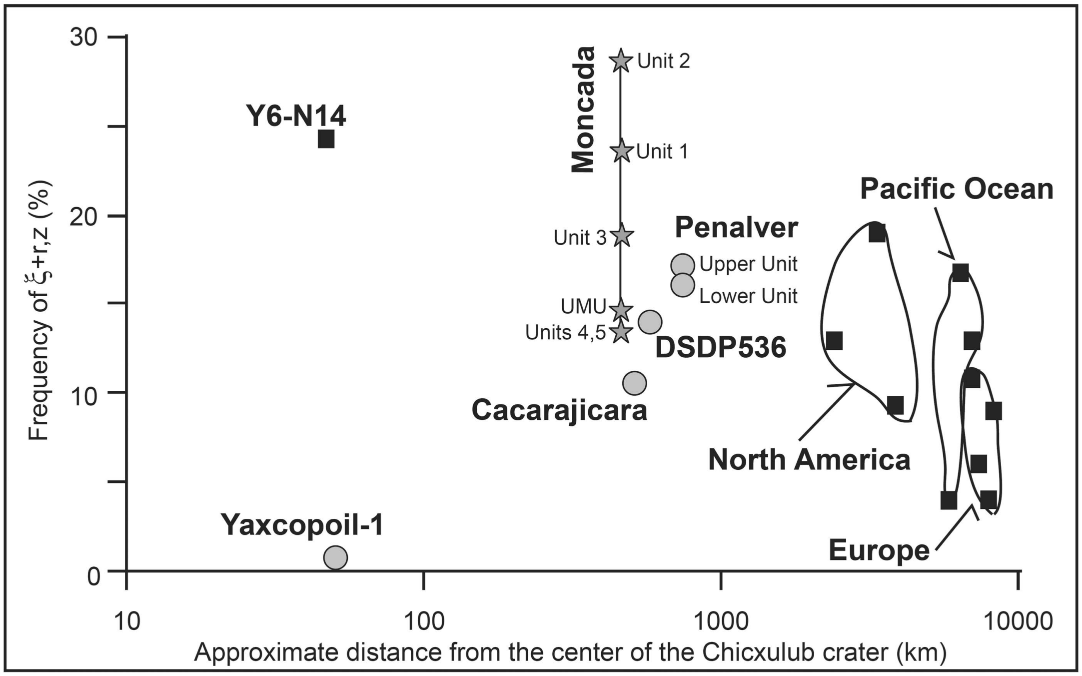

Fig. 10. Frequency of PDFs with ξ $\{11\bar{2}2\}$ plus r, z $\{10\bar{1}1\}$ orientation is plotted against the distance from the center of the Chicxulub crater.

$\{10\bar{1}1\}$ orientations tends to decrease with the increase in distance from the crater except for the sample from the YAX-1 core (Fig. 10). The frequency of PDFs with ξ $\{11\bar{2}2\}$ plus r, z $\{10\bar{1}1\}$ decreases at more distal sites; namely 10–20% at north American sites, 5–15% at Pacific Ocean sites, and less than 10% at European sites (Fig. 10). On the other hand, our preliminary measurements of PDF orientations in shocked quartz grains at the diamictite bed of the Albion Formation, Belize and Mexico, one of the closest K/T boundary ejecta blanket deposit at a distance of approximately 350 km from the crater center (Ocampo et al. 1996; Pope et al. 1999), show 35% of PDFs with ξ $\{11\bar{2}2\}$ plus r, z $\{10\bar{1}1\}$ orientations (Nakano et al. 2005).

According to Robertson and Grieve (1977), PDFs with ξ $\{11\bar{2}2\}$ plus r, z $\{10\bar{1}1\}$ orientations are formed around 15 GPa (Table 1). Therefore, abundant occurrence of PDFs with ξ $\{11\bar{2}2\}$ plus r, z $\{10\bar{1}1\}$ probably indicates that shocked quartz grains in the proximity of the crater were mainly derived from the shock pressure zone around 15 GPa. Alternatively, planar deformation features with ξ $\{11\bar{2}2\}$ plus r, z $\{10\bar{1}1\}$ orientations are frequently observed at craters formed in a porous sedimentary target (e.g., French et al. 1974; Grieve et al. 1996). According to the experimental results by Nakano et al. (2002), PDFs with ξ $\{11\bar{2}2\}$ plus r, z $\{10\bar{1}1\}$ orientations are prominent for porous quartz sand targets at relatively low shock pressure (14–20 GPa), whereas they are rarely observed above 20 GPa. Thus, abundant occurrence of PDFs with ξ $\{11\bar{2}2\}$ plus r, z $\{10\bar{1}1\}$ around the crater might reflects that there were porous sedimentary rocks around the impact target, although this idea has to be confirmed by more data.

On the other hand, PDFs with ξ $\{11\bar{2}2\}$ plus r, z $\{10\bar{1}1\}$ orientation are rarely observed in the sample from the YAX-1 core. Because PDFs with ξ $\{11\bar{2}2\}$ plus r, z $\{10\bar{1}1\}$ orientation are rarely observed above 20 GPa both at crystalline and porous targets (e.g., Stöffler and Langenhorst 1994; Nakano et al. 2002), shocked quartz grains in the YAX-1 core sample were probably derived from the HSPZ of more than 20 GPa. Although further investigation is required, this interpretation is consistent with the observation that the occurrence of PDFs with c(0001) orientation is rare in this sample, whereas occurrence of π $\{10\bar{1}2\}$ orientation, which is formed under the highest shock pressure (>23 GPa), is abundant (20%).

Variation of PDF Orientations and Grain Size Distribution Over the Moncada Formation

Here, we discuss the variation of PDF orientations of shocked quartz grains over the Moncada Formation. The Moncada Formation was probably formed at a water depth greater than 200 m under the influence of the repeated tsunamis due to the impact (Tada et al. 2002). Therefore, deposition of shocked quartz grains might have been complex due to the tsunami agitation. However, because there is no erosional surface in each unit boundary of the Moncada Formation (Tada et al. 2002), shocked quartz grains once deposited in each unit could not have been resuspended by the subsequent tsunami waves.

Our data shows that frequency of PDFs with ξ $\{11\bar{2}2\}$ plus r, z $\{10\bar{1}1\}$ orientations is high in the lower part of the Moncada Formation, but it decreases upward (Fig. 4). On the contrary, PDFs with π $\{10\bar{1}2\}$ orientation increase upward from units 1 to 4 + 5, although they are very rare in the UMU (Fig. 4). This inversely related trend probably reflects the variation of relative abundance of shocked quartz grains derived from the LSPZ and HSPZ through the Moncada Formation; namely, shocked quartz grains from the LSPZ are abundant in the lower part, whereas those from the HSPZ are abundant in the upper part of the Moncada Formation. On the other hand, PDFs with π $\{10\bar{1}2\}$ orientation are extremely rare in the UMU (Fig. 4). The sample from the UMU was taken from the olive-gray fine sandstone layer above the Ir-bearing claystone layer in the UMU and is interpreted as the reworked layer formed during the settling of Ir-bearing particles (Tada et al. 2002). Therefore, the shocked quartz grains in this sample could represent a mixture of shocked quartz from various sources deposited around the Moncada Formation.

CONCLUSION

We have investigated PDF orientations in quartz grains at 5 sites within approximately 800 km of the crater center of Chicxulub. We found that PDFs with c(0001) and ξ $\{11\bar{2}2\}$ plus r, z $\{10\bar{1}1\}$ orientations are distributed differently in the different types of ejecta deposits with respect to the depositional horizon and distance from the Chicxulub crater. Variations of these orientations probably reflect which material from the different shock pressure levels during the impact was comprised in the ejection processes. We also have investigated the variation of PDF orientations in quartz grains in the Moncada Formation and found that the lower part of the formation tends to contain shocked quartz grains derived from the low-pressure zone, whereas the upper part contains those from the high-pressure zone. Further measurements of PDF orientations in quartz as well as the abundance and grain size of shocked quartz in the K/T boundary deposits, especially in NE Mexico, the Atlantic Ocean, and Southern Hemisphere, where no information on PDF orientations is published so far, will help to understand more details of the Chicxulub impact process including heterogeneity of the ejecta distribution and impact angle.

Acknowledgments—Part of the samples and data was provided by the International Continental Scientific Drilling Program and the Ocean Drilling Program. We wish to thank curatorial support for sampling by J. U. Fucugauchi at Universidad Nacional Autónoma de México, and by G. Esmay at East Coast Repository. We also thank A. Deutsch, Ph. Claeys, J. Morrow, S. Kiyokawa, and S. Sugita for their valuable suggestions and comments. The research was supported by research funds donated to the University of Tokyo by T. Yoda and in part by a Grant-in-Aid for Scientific Research from the Japan Society for the Promotion of Science (no. 17403005).

Editorial Handling—Dr. Alexander Deutsch

REFERENCES

Alexopoulos J. S., Grieve R. A. F., and Robertson P. B. 1988. Microscopic lamellar deformation features in quartz: Discriminative characteristics of shock-generated varieties. *Geology* 16:796–799.

Alvarez W., Smit J., Lowrie W., Asaro F., Margolis S. L., Claeys Ph., Kastner M., and Hildebrand A. R. 1992. Proximal impact deposits at the Cretaceous-Tertiary boundary in the Gulf of Mexico: A re-study of DSDP leg 77 Site 536 and 540. *Geology* 20:697–700.

Alvarez W., Claeys Ph., and Kieffer S. W. 1995. Emplacement of K/T boundary shocked quartz from Chicxulub crater. *Science* 269: 930–935.

Badjukov D. D., Nazarov M. A., and Suponeva I. V. 1986. Shocked quartz grains from K/T boundary sediments (abstract). 18th Lunar and Planetary Science Conference. pp. 18–19.

Bohor B. F. 1990. Shock-induced microdeformations in quartz and other mineralogical indications of an impact event at the Cretaceous/Tertiary boundary. *Tectonophysics* 171:359–372.

Bohor B. F., Foord E. E., Modereski P. J., and Triplehorn D. M. 1984. Mineralogic evidence for an impact event at the Cretaceous-Tertiary boundary. *Science* 224:867–869.

Bohor B. F., Moderski P. J., and Foord E. E. 1987. Shocked quartz in the Cretaceous-Tertiary boundary clays: Evidence for a global distribution. *Science* 236:705–709.

Bostwick J. A. and Kyte F. T. 1996. The size abundance of shocked quartz in Cretaceous-Tertiary boundary sediments from the Pacific Basin. In: *Cretaceous-Tertiary event and other catastrophes in earth history*, edited by Ryder G., Fastovsky D. and Gartner S. Special Paper #307. Boulder, Corolado: Geological Society of America. pp. 403–415.

Bralower T. J., Paul C. K., and Leckie R. M. 1998. The Cretaceous/Tertiary boundary cocktail: Chicxulub impact triggers margin collapse and extensive sedimentary gravity flows. *Geology* 26: 331–334.

Brönnimann P. and Rigassi D. 1963. Contribution to geology and paleontology of area of the city of La Habana, Cuba, and its surroundings. *Eclogae Geologicae Helvetiae* 56:193–480.

Buffler R. T. et al. 1984. *Initial reports, Deep-Sea Drilling Project*, vol. 77. Washington, D.C.: U.S. Government Printing Office. p. 747.

Claeys Ph. 2006. Chicxulub, anatomy of a multi-ring basin: From impactite formation to ejecta distribution (abstract #368081). First International Conference on Impact Cratering in the Solar System 1. CD-ROM.

Claeys Ph., Kiessling W., and Alvarez W. 2002. Distribution of Chicxulub ejecta at the Cretaceous-Tertiary boundary. In: *Catastrophic events and mass extinctions: Impact and beyond*, edited by Koeberl C. and MacLeod G. GSA Special Paper #356. Boulder, Corolado: Geological Society of America. pp. 55–68.

Claeys Ph., Heuschkel S., Lounejeva-Baturina E., Sanchez-Rubio G., and Stöffler D. 2003. The suevite of drill hole Yucatán 6 in the Chicxulub impact crater. *Meteoritics & Planetary Science* 38:1299–1317.

DeCarli P. S. and Jamieson J. C. 1959. Formation of an amorphous form of quartz under shock conditions. *Journal of Chemical Physics* 31:1675–1676.

Dressler B. O., Sharpton V. L., Schwandt C. S., and Ames D. 2004. Impactites of the Yaxcopoil-1 drilling site, Chicxulub impact structure: Petrography, geochemistry, and depositional environment. *Meteoritics & Planetary Science* 39:857–878.

French B. M. and Short N. M., eds. 1968. *Shock metamorphism of natural materials*. Baltimore: Mono Book Corporation. 644 p.

French B. M., Underwood J. R., and Fisk R. P. 1974. Shock metamorphic features in two meteorite impact structures, southeastern Libya. *Geological Society of America Bulletin* 85: 1425–1428.

Goto K., Nakano Y., Tajika E., Tada R., Iturralde-Vinent M. A., and Matsui T. 2002. Constraint on the depositional process of the K/T boundary proximal deep-sea deposit in northwestern Cuba based on shocked quartz distribution and its grain size (abstract). 34th Annual Meeting of the Geological Society of America. p. 239.

Goto K., Tada R., Tajika E., Bralower T. J., Hasegawa T., and Matsui T. 2004. Evidence for ocean water invasion into the Chicxulub crater at the Cretaceous/Tertiary boundary. *Meteoritics & Planetary Science* 39:1233–1247.

Goto K., Tada R., Tajika E., Iturralde-Vinent M. A., Matsui T., Yamamoto S., Nakano Y., Oji T., Kiyokawa S., Garcia D., Otero C., Rojas R. 2008. Lateral lithological and compositional variations of the Cretaceous/Tertiary deep-sea tsunami deposit in northwestern Cuba. *Cretaceous Research* 29:217–236.

Gratz A. J., Fisler D. K., and Bohor B. F., 1996. Distinguishing shocked from tectonically deformed quartz by the use of the SEM and chemical etching. *Earth and Planetary Science Letters* 142: 513–521.

Grieve R. A. F. and Robertson P. B. 1976. Variations in shock deformation at the Slate Island impact structure, Lake Superior, Canada. *Contribution to Mineralogy and Petrology* 58:37–49.

Grieve R. A. F. and Alexopoulos J. 1988. Microscopic planar features in quartz from Scollard Canyon, Alberta, and the Cretaceous-Tertiary boundary event. *Canadian Journal of Earth Science* 25: 1530–1534.

Grieve R. A. F., Langenhorst F., and Stöffler D. 1996. Shock metamorphism of quartz in nature and experiment II: Significance in geoscience. *Meteoritics & Planetary Science* 31:6–35.

Hörz F. 1968. Statistical measurements of deformation structures and refractive indices in experimentally shock loaded quartz. In *Shock metamorphism of natural materials*, edited by French B. M. and Short N. M. Baltimore: Mono Book Corporation. pp. 243–253.

Iturralde-Vinent M. A. 1994. Cuban geology: A new plate-tectonic synthesis. *Journal of Petroleum Geology* 17:39–70.

Iturralde-Vinent M. A. 1998. Sinopsis de la constitución geológica de Cuba. In *Geología y metalogénia de Cuba: Una introducción*, edited by Melgarejo J. C. and Proenza J. A. *Acta Geologica Hispánica* 33:9–56.

Izett G. A. 1990. *The Cretaceous/Tertiary boundary interval, Raton Basin, Colorado and New Mexico*. GSA Special Paper #249. Boulder, Colorado: Geological Society of America. 100 p.

Kiyokawa S., Tada R., Iturralde-Vinent M. A., Tajika E., Yamamoto S., Oji T., Nakano Y., Goto K., Takayama H., Garcia-Deogado D., Diaz-Otero C., Rojas-Consuegra R., and Matsui T. 2002. Cretaceous-Tertiary boundary sequence in the Cacarajícara Formation, western Cuba: An impact-related, high-energy, gravity-flow deposit. In *Catastrophic events and mass extinctions: Impact and beyond*, edited by Koeberl C. and MacLeod K. G. GSA Special Paper #356. Boulder, Colorado: Geological Society of America. pp. 125–144.

Kring D. A., Hildebrand A. R., and Boynton W. V. 1994. Provenance of mineral phases in the Cretaceous-Tertiary boundary sediments exposed on the southern peninsula of Haiti. *Earth and Planetary Science Letters* 128:629–641.

Kring D. A., Hörz F., Zurcher L., and Urrutia-Fucugauchi J. 2004. Impact lithologies and their emplacement in the Chicxulub impact crater: Initial results from the Chicxulub Scientific Drilling Project, Yaxcopoil, Mexico. *Meteoritics & Planetary Science* 39: 879–897.

Langenhorst F. 1994. Shock experiments on pre-heated α- and β-quartz: II. X-ray and TEM investigations. *Earth and Planetary Science Letters* 128:683–698.

Langenhorst F. 2002. Shock metamorphism of some minerals: Basic introduction and microstructural observations. *Bulletin of the Czech Geological Survey* 77:265–282.

Langenhorst F. and Deutsch A. 1994. Shock experiments on pre-heated α- and ß-quartz: I. Optical and density data. *Earth and Planetary Science Letters* 125:407–420.

Leroux H., Rocchia R., Froget L., Orue-Etxebarria X., Doukhan J. C., and Robin E. 1995. The K/T boundary at Beloc (Haiti): Compared stratigraphic distributions of the boundary markers. *Earth and Planetary Science Letters* 131:255–268.

Melosh H. J. 1989. *Impact cratering: A geological process*. Oxford: Oxford University Press. p. 245.

Morgan J., Lana C., Kearsley A., Coles B., Belcher C., Montanari S., Diaz-Martinez E., Barbosa A., and Neumann V. 2006. Analyses of shocked quartz at the global K-P boundary indicate an origin from a single, high-angle, oblique impact at Chicxulub. *Earth and Planetary Science Letters* 251:264–279.

Morrow J. R. and Sandberg C. A. 2001. Distribution and characteristics of multi-sourced shock-metamorphosed quartz grains, Late Devonian Alamo impact, Nevada (abstract #1080). 32nd Lunar and Planetary Science Conference. CD-ROM.

Nakano Y., Hasegawa S., Sugita S., Fujiwara A., and Matsui T. 2002. An experimental study on the shock metamorphism of quartz sand. Proceedings, 35th ISAS Lunar and Planetary Symposium. pp. 158–161.

Nakano Y., Goto K., Matsui T., Tada T., and Tajika E. 2005. Shocked quartz distribution inside and outside the Chicxulub crater (abstract). *Geological Society of America Abstracts with Programs* 37:287.

Ocampo A. C., Pope K. O., and Fischer A. G. 1996. Ejecta blanket deposit of the Chicxulub crater from Albion Island, Belize. In: *Cretaceous-Tertiary event and other catastrophes in Earth history*, edited by Ryder G., Fastovsky D., and Gartner S. GSA Special Paper #307. Boulder, Colorado: Geological Society of America. pp. 75–88.

Pindell J. 1994. Evolution of the Gulf of Mexico and the Caribbean. In *Caribbean geology, an introduction*, edited by Donovan S. K. and Jackson T. A. Kingston: University of the West Indies Publishers Association. pp. 13–40.

Pope K. O., Ocampo A. C., Fischer A. G., Alvarez W., Fouke B. W., Webster C. L., Vega F. J., Smit J., Fritsche A. E., and Claeys Ph. 1999. Chicxulub impact ejecta from Albion Island, Belize. *Earth and Planetary Science Letters* 170:351–364.

Pszczółkowski A. 1987. Paleogeography and tectonic evolution of Cuba and adjoining areas during the Jurassic-Early Cretaceous. *Annales Societatis Geologorum Poloniae* 57:127–142.

Pszczółkowski A. 1999. The exposed passive margin of North America in western Cuba. In *Caribbean basins (Sedimentary basins of the world),* edited by Mann P. Amsterdam: Elsevier. pp. 93–121.

Robertson P. B. and Grieve R. A. F. 1977. Shock attenuation at terrestrial impact structures. In *Impact and explosion cratering*, edited by Roddy D. J., Pepin R. O., and Merrill R. B. New York: Pergamon Press. pp. 687–702.

Rosencrantz E. 1990. Structure and tectonics of the Yucatán Basin, Caribbean Sea, as determined from seismic reflection studies. *Tectonics* 9:1037–1059.

Sharpton V. L. and Grieve R. A. F. 1990. Meteorite impact, cryptoexplosion, and shock metamorphism: A perspective on the evidence at the K/T boundary. In *Global catastrophes in Earth history*, edited by Sharpton V. L. and Ward P. D. GSA Special

Paper #247. Boulder, Colorado: Geological Society of America. pp. 301–318.
Sharpton V. L., Dalrymple G. B., Marin L. E., Ryder G., Schuraytz B. C., and Urrutia-Fucugauchi J. 1992. New links between the Chicxulub impact structure and the Cretaceous/Tertiary boundary. *Nature* 359:819–821.
Smit J. 1999. The global stratigraphy of the Cretaceous-Tertiary boundary impact ejecta. *Annual Review of Earth and Planetary Science* 27:75–113.
Smit J., Montanari A., Swinburne N. H. M., Alvarez W., Hildebrand A. R., Margolis A. V., Claeys Ph., Lowrie W., and Asaro F. 1992. Tektite-bearing, deep-water clastic unit at the Cretaceous-Tertiary boundary in northeastern Mexico. *Geology* 20:99–103.
Smit J., Gaast S. V. D., and Lustenhouwer W. 2004. Is the transition impact to post-impact rock complete? Some remarks based on XRF scanning, electron microprobe, and thin section analyses of the Yaxcopoil-1 core in the Chicxulub crater. *Meteoritics & Planetary Science* 39:1113–1126.
Stöffler D. 1972. Deformation and transformation of rock-forming minerals by natural and experimental shock processes 1. Behavior of minerals under shock compression. *Fortschritte der Mineralogie* 49:50–113.
Stöffler D. 1974. Deformation and transformation of rock-forming minerals by natural and experimental shock processes 2. Physical properties of shocked minerals. *Fortschritte der Mineralogie* 51: 256–289.
Stöffler D. and Langenhorst F. 1994. Shock metamorphism of quartz in nature and experiment: I. Basic observation and theory. *Meteoritics* 29:155–181.
Stöffler D., Artemieva N., Ivanov B., Hecht L., Kenkmann T., Schmitt R., Tagle R., and Wittmann A. 2004. Origin and emplacement of the impact formations at Chicxulub, Mexico, as revealed by the ICDP deep drilling at Yaxcopoil-1 and by numerical modeling. *Meteoritics & Planetary Science* 39:1035–1067.
Tada R., Nakano Y., Iturralde-Vinent M. A., Yamamoto S., Kamata K., Tajika E., Toyoda K., Kiyokawa S., Garcia-Delgado D., Oji T., Goto K., Takayama H., Rojas-Consuegra R., and Matsui T. 2002. Complex tsunami waves suggested by the Cretaceous-Tertiary boundary deposit at the Moncada section, western Cuba. In: *Catastrophic events and mass extinctions: Impact and beyond*, edited by Koeberl C., and MacLeod G. GSA Special Paper #356. Boulder, Colorado: Geological Society of America. pp. 109–123.
Tada R., Iturralde-Vinent M. A., Matsui T., Tajika E., Oji T., Goto K., Nakano Y., Takayama H., Yamamoto S., Kiyokawa S., Toyoda K., Garcia-Delgado D., Diaz-Otero C., and Rojas-Consuegra R. 2003. K/T boundary deposit in the proto-Caribbean Basin. *Memoir American Association of Petroleum Geologists* 79:582–604.
Takayama H., Tada R., Matsui T., Iturralde-Vinent M. A., Oji T., Tajika E., Kiyokawa S., Garcia D., Okada H., Hasegawa T., and Toyoda K. 2000. Origin of the Peñalver Formation and its relation to K/T boundary impact event. *Sedimentary Geology* 135:295–320.
Tuchscherer M. G., Reimold W. U., Koeberl C., Gibson R. L., and Bruin D. D. 2004. First petrographic results on impactites from the Yaxcopoil-1 borehole, Chicxulub structure, Mexico. *Meteoritics & Planetary Science* 39:899–930.
Vernooij M. G. C. and Langenhorst F. 2005. Experimental reproduction of tectonic deformation lamellae in quartz and comparison to shock-induced planar deformation features. *Meteoritics & Planetary Science* 40:1353–1361.